Biomed Microdevices (2013) 15:1–8
DOI 10.1007/s10544-012-9681-4

Bubble Jet agent release cartridge for chemical single cell stimulation

N. Wangler · M. Welsche · M. Blazek · M. Blessing · M. Vervliet-Scheebaum · R. Reski · C. Müller · H. Reinecke · J. Steigert · G. Roth · R. Zengerle · N. Paust

Published online: 26 July 2012

Abstract We present a new method for the distinct specific chemical stimulation of single cells and small cell clusters within their natural environment. By single-drop release of chemical agents with droplets in size of typical cell diameters (d <30 μm) on-demand micro gradients can be generated for the specific manipulation of single cells. A single channel and a double channel agent release cartridge with integrated fluidic structures and integrated agent reservoirs are shown, tested, and compared in this publication. The single channel setup features a fluidic structure fabricated by anisotropic etching of silicon. To allow for simultaneous release of different agents even though maintaining the same device size, the second type comprises a double channel fluidic structure, fabricated by photolithographic patterning of TMMF. Dispensed droplet volumes are V=15 pl and V= 10 pl for the silicon and the TMMF based setups, respectively. Utilizing the agent release cartridges, the application in biological assays was demonstrated by hormone-stimulated premature bud formation in *Physcomitrella patens* and the individual staining of one single L 929 cell within a confluent grown cell culture.

Keywords Single cell stimulation · Drop-on-demand · InkJet · Agent release · Pyscomitrella patens · L-929

Electronic supplementary material The online version of this article (doi:10.1007/s10544-012-9681-4) contains supplementary material, which is available to authorized users.

N. Wangler · M. Welsche · M. Blazek · R. Reski · J. Steigert · G. Roth · R. Zengerle
BIOSS – Centre for Biological Signalling Studies,
University of Freiburg,
Freiburg, Germany

N. Wangler (✉) · M. Welsche · M. Blazek · R. Zengerle · N. Paust
Laboratory for MEMS Applications, Department of Microsystems Engineering – IMTEK, University of Freiburg,
Freiburg, Germany
e-mail: nicolai.wangler@imtek.uni-freiburg.de

C. Müller · H. Reinecke
Laboratory for Process Technology, Department of Microsystems Engineering – IMTEK, University of Freiburg,
Freiburg, Germany

M. Blessing · M. Vervliet-Scheebaum · R. Reski
Plant Biotechnology, Faculty of Biology, University of Freiburg,
Freiburg, Germany

R. Reski
FRIAS – Freiburg Institute for Advanced Studies,
University of Freiburg,
Freiburg, Germany

1 Introduction

The highly promising possibility of chip based cell analysis has caused a considerable increase of research and development on cells over the last few years (Andersson and van den Berg 2004; Andersson and van den Berg 2007). One focus of interest aims for the stimulation or manipulation of single cells. Thereby, cells are mainly stimulated and measured by electrical systems like Patch-Clamp or multi electrode arrays (MEAs) (Jonas et al. 1995; Egert et al. 1998; Wagenaar et al. 2004; Dadacz-Narloch et al. 2011). Unlike specific chemical stimulation, electrical cell stimulation is mainly unspecific and can lead to cell damage over time (Liu et al. 1999). By using chemical stimulation, signaling pathways can be triggered selectively which marks a definite advantage in stimulating complex organs e.g. by mimicking a synapse with an artificial system (Noolandi et al.

2003). For this purpose, the generation of biomolecular gradients plays a major role (Keenan and Folch 2008) to mimic nature-like conditions.

Various approaches for the generation of biochemical gradients and thus for stimulation of the cells have been presented in the past (Boyden 1962; El-Ali et al. 2005; Peterman et al. 2004; Takayama et al. 2001; Eppendorf et al. 2011; Cellectricon et al. 2011). The microfluidic devices can be separated into two categories, (a) laminar flow systems, and (b) pulsed release of stimulating agents.

1.1 Laminar flow systems

The theta-glass capillary, a two channel glass capillary with a cross-section that looks like the Greek letter theta θ, has become a standard tool in neuroscience (Jonas et al. 1995). A very sharp interface is built between two laminar flowing solutions ejected by the two cavities where an isolated cell can be positioned. Fast piezo driven deflections of the theta-glass capillary or the cell itself lead to short stimulation times (Jonas et al. 1995). A chip-based variation of this method is commercialized by *Cellectricon*® (Cellectricon et al. 2011). Here, the patched cell is moved through up to 16 different media by a micromanipulator.

However, for laminar flow systems, isolated cells (Takayama et al. 2001) or cell clusters (Kraus et al. 2006) and liquid interface have to be aligned to each other.

The most challenging drawback of laminar flow systems is that they require large quantities of biochemical agents due to the continuous flow regime which may increase the costs drastically.

1.2 Pulsed agent release

To reduce the quantities of biochemical agents, it is self-evident to reduce the volumes and release the stimuli on demand, only. So-called micro injectors like the *FemtoJet*® setup presented by *Eppendorf*® (Eppendorf et al. 2011) allow for the precise agent release (V=0.1–100 pl) through a thin capillary with diameters between 0.5 and 1 μm positioned into or next to a target cell. Using multi-barrel capillaries multiple drugs can be released. Due to the high fluidic resistance of the extremely small channels, the injection process is quite slow and additional handling steps as degassing or filtering of the liquids are necessary as well (Jonas et al. 1995). Additionally, the prevention of clogging requires elaborate liquid preparation. Thus, the use of these systems is more or less restricted to specialized applications like direct injections into cells or cells' nuclei exchange, e.g. in the field of stem cell research.

In other approaches, the bottom of the cell culture dish is replaced by porous membranes or other release apertures (Peterman et al. 2004; Leoni et al. 2002; Zibek et al. 2006) to stimulate at the bottom adherent cells. Typically, the released drug has to diffuse to the target cells, randomly distributed around the release sites.

1.3 Pulsed agent release by InkJet technology

Since the invention of the InkJet printing technology in the early 1950s (Elmqvist et al. 1951), much progress has been made in delivering discrete and controlled volumes of liquids to defined locations – also known as drop-on-demand printing. In the 1980s, the thermally actuated InkJet printing technology (Bubble-Jet) was invented by *Canon*® and *Hewlett-Packard*® (Le 1998). This technology utilizes a fast expanding gas bubble, generated by a heat actuation unit, to eject free flying droplets (see Fig. 1(a)).

Its semiconductor compatible fabrication and the low installation size paved the way for becoming a key player in InkJet dispensing. Nowadays, InkJet technology and in particular thermal InkJet printing is more and more applied in biological experiments (Zibek et al. 2006; Boland et al. 2006; Roth et al. 2004). By releasing small droplets in a range of a few picolitres, temporal micro-gradients can be achieved similar to the applications of pulsed agent release as mentioned before. Cells can be exposed to these gradients by patch clamp pipette, for example.

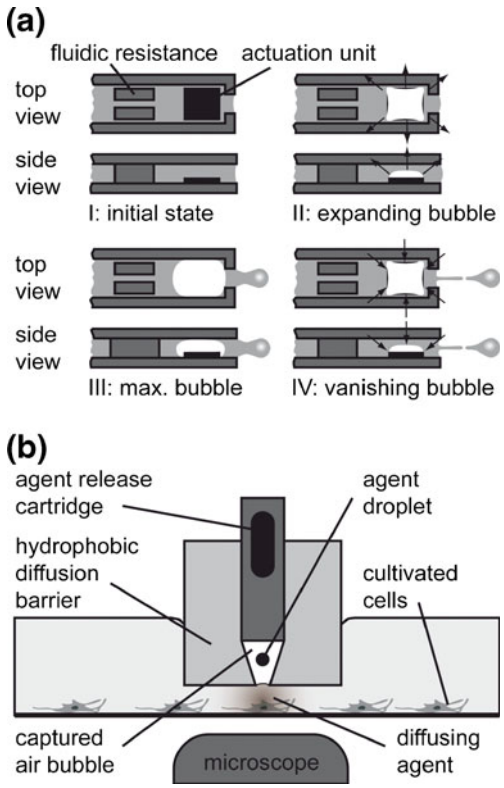

Fig. 1 Schematic diagram of the experimental setup. (**a**) Schematic of the Bubble-Jet actuation principle. (**b**) Experimental setup for single cell stimulation

Nevertheless, it has to be considered that for all pulsed agent release applications, diffusion based leakage challenges the distinct release of liquid agent when the release unit is inserted into a liquid target medium.

In this publication we present the development and application of small sized needle-like Bubble-Jet actuated agent release cartridges, comprising integrated fluidic reservoirs. The cartridges can be positioned to individually selected cells as depicted in Fig. 1(b). Thus, there is no need of moving the cells into a stimulation environment.

The application of a hydrophobic diffusion barrier ensures a stable phase separation between agent and liquid target medium by capturing an air bubble in front of the nozzle orifice. Dispensed agent droplets transcend this air bubble by flying through it as we've presented by our previous work (Steigert et al. 2009). The diffusion barrier allows for utilization of the cartridge within liquid environments without any diffusion based leakage.

The presented cartridges are applied in two biological applications: (a) distinct modification of moss protonema cells and (b) specific staining of a single cell within a confluent grown cell culture.

Fig. 2 Photograph picture of the two presented agent release cartridges. The lower tool is the single channel agent release cartridge, the upper one the double channel agent release cartridge. The diameter of the coin is d=16.25 mm

2 Agent release cartridges

Two different types of the agent release cartridges are presented within this publication.

Thereby, the first kind, the single channel agent release cartridge comprises a sandwich of a Pyrex glass substrate which features the Bubble-Jet actuation unit and a silicon based substrate featuring anisotropically etched fluidic structures. The two substrates are combined by anodic bonding of silicon and Pyrex. With geometric dimensions of 10×1.5×1 mm³ (length × width × height), the agent release cartridge features an integrated reservoir with a reservoir volume of V=1 µl. A 20×25 µm² nozzle with a nozzle length of 50 µm is located at the front edge of the cartridge. Illustrated by the lower tool in Fig. 2, the single channel agent release cartridge with its front edge facing to the right side is depicted.

For some biological applications, the availability of several individually addressable channels is desirable. For example, staining might be performed in parallel to stimulation protocols using two individual channels. For this purpose, further miniaturization of the agent release cartridge is desirable.

Therefore we present the second kind, an 8×1.4×0.7 mm³ (length × width × height) large double channel agent release cartridge (see upper tool in Fig. 2) that allows for the individually addressable actuation of two separated channels. Thereby, the two nozzles feature a distance of $d_{nozzle\text{-}nozzle}$=100 µm. The double channel agent release cartridge comprises a silicon base-substrate, featuring the Bubble-Jet actuation units as well as anisotropically etched fluidic reservoirs. Fluidic structures and their sealing are realized by lamination and structuring of the epoxy-based photostructable dry-film resist TMMF (Stöhr et al. 2008; Wangler et al. 2011).

2.1 Fabrication process

The fabrication of the Bubble-Jet actuation units starts with (Ia/i) the deposition of 200 nm of silicon nitride for chemical passivation (diffusion barrier) of the Pyrex glass substrate (in case of the single channel release cartridge) and for chemical and electrical passivation of the silicon base-substrate (in case of double channel agent release cartridge) as illustrated in Fig. 3. Titanium (100 nm) and aluminum (600 nm) are evaporated as heater material and conduction layer (IIa/ii) and structured via lift-off afterwards. After opening the heater area of (35×35 µm²) by means of (IIIa/iii) chemical wet etching of aluminum, the whole metallization is (IVa/iv) passivated by a second layer of silicon nitride (800 nm). Bondpads are opened via reactive ion etching (RIE) of the covering silicon nitride and finally, in case of the single channel agent release cartridge, the surrounding silicon nitride layers are (Va) etched via RIE as well to enable anodic bonding with the silicon based top-substrate.

For the fabrication of the single channel agent release cartridge, the top-substrate is structured by deep reactive ion etching (DRIE) of silicon from both sides of the wafer (compare Fig. 3(a)). Starting with (Ib) marking and alignment structures on the wafer top side, fluidic channels and nozzles are (IIb) structured from the backside of the wafer. Thereby a depth of the fluidic channel and the 20 µm wide nozzle of $h_{channel}$=25 µm is kept. The Bubble-Jet actuation chamber features a size of 100×60×25 µm³. After patterning the fluidic structures, a layer (IIIb) of silicon oxide

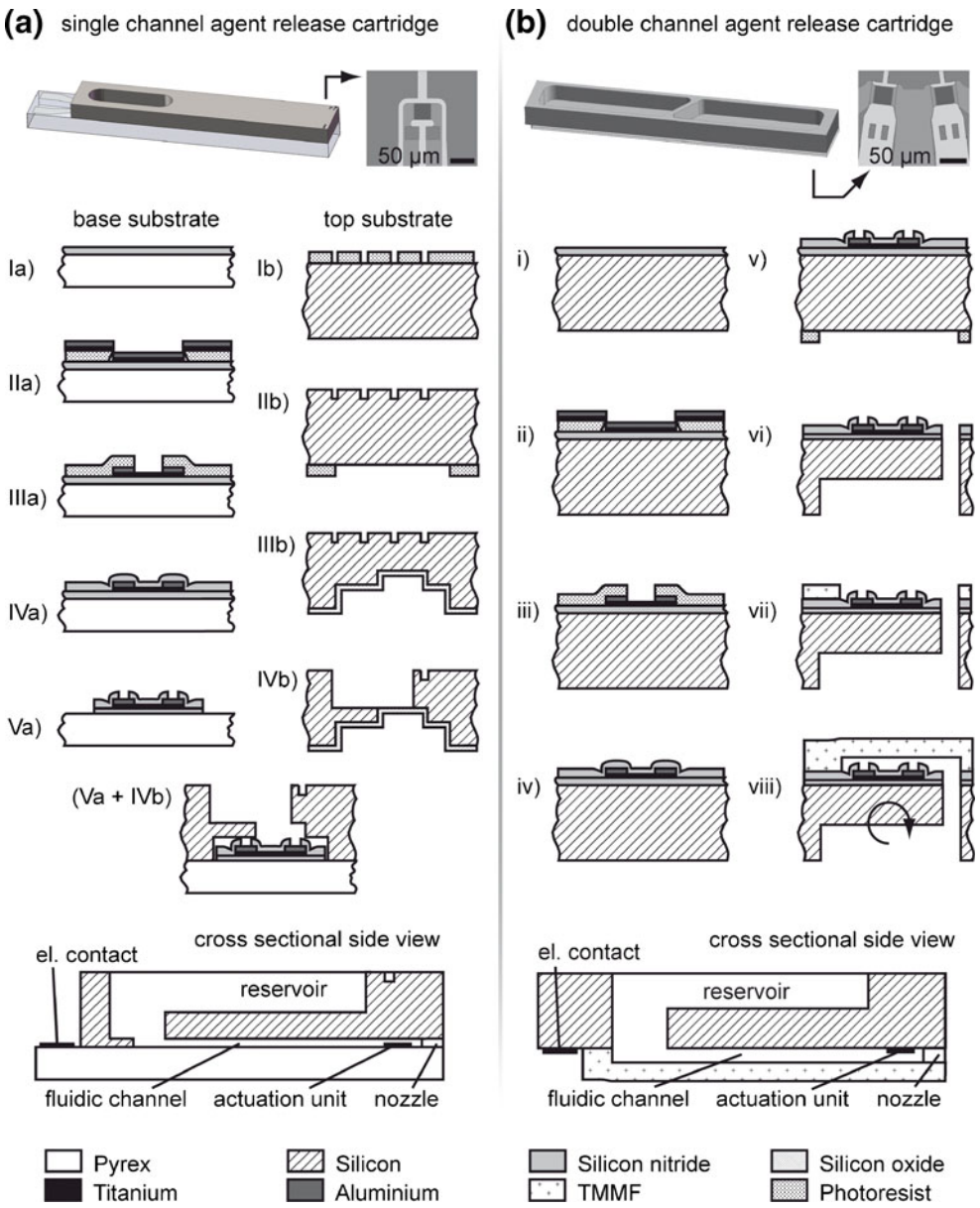

Fig. 3 Fabrication scheme of the agent release cartridge. (**a**) Depicts the fabrication of the single channel agent release cartridge, based on anodic bonding of Pyrex glass base-substrate featuring the actuation unit and a silicon top-substrate featuring fluidic channels and the reservoir. (**b**) Depicts the fabrication of the double channel agent release cartridge, based on a silicon base-substrate featuring actuation unit and the reservoirs and fluidic channels made of TMMF dry film resist polymer

smoothens the fluidic structures and acts as an etch stop layer for (IVb) the structuring of the fluidic reservoir.

Subsequently to the reservoir patterning, the silicon oxide layer is removed again and base and top-substrate are bonded via anodic bonding on wafer level. Finally, a dicing procedure separates the agent release cartridges and thereby opens the nozzle which is located perpendicular to the heater structure. The nozzle length is thereby supposed to be l_{nozzle}=50 µm.

In case of the double channel agent release cartridge fabrication (Fig. 3(b)), (v) fluidic reservoirs and (vi) vias to the metallized front side are etched into the bulk silicon via DRIE. After removing the silicon nitride layer at the fluidic vias, a layer of TMMF dry-film resist is laminated onto the Bubble-Jet heater structures of the patterned base-material (vii). The 30 µm thick epoxy-based dry-film photoresist TMMF S2030 of Tokyo Ohka Kogyo Co., Ltd. is sold as lamination-able high contrast and at the line of near ultraviolet (UV) radiation sensitive polymer substrate, showing excellent optical properties, as well as a good chemical resistivity TMMF (Stöhr et al. 2008; Wangler et al. 2011). It features an appropriate resolution (w_{min} <10 µm) with an obtainable aspect ratio of 9 : 2 (height : width). The TMMF dry-film resist is patterned by UV lithography to realize the 30 µm deep fluidic channels, the 50×50×30 µm³ large Bubble-Jet actuation chamber, and the 15 µm wide nozzle structures. By lamination of a second layer TMMF (TMMF S2055), the fluidic channel structures are (viii) finally sealed, utilizing an adapted fabrication process as presented in (Wangler et al. 2011). Afterwards, the chips are separated by the subsequent dicing procedure, similar to the fabrication of the single channel approach.

2.2 Characterization

The presented single channel agent release cartridge features the typical characteristics and droplet tear-off behavior of commercial Bubble-Jet printheads, dispensing deionized water by using our standard actuation protocol (see table 1). By gravimetrical measurement of 1,000 shot salves of deionized water, an average droplet volume of V_{drop}=15.1 pl was determined. Thereby the masses of the salves from one single dispenser deviate not exceeding a variation coefficient (CV) of CV=4.4 % within a maximum range of $V_{drop,max}$-$V_{drop,min}$=1.8 pl.

A deflection of the sawing path for opening the nozzle structure (Δs~5 μm dicing tolerance, Disco DAD 321) results directly in a variation of the nozzle length which is in turn correlated to the dispensed droplet volume due to the change of the fluidic resistance of the nozzle structure. In all probability, the identified deviation of the dispensed droplet volume of five exemplary cartridges (CV=12 %) is caused by the dicing accuracy.

The double channel agent release cartridge features as well the typical dispensing characteristics of commercial Bubble-Jet dispensers but the polymer based fluidic structure in TMMF dry-film resist does not reach the high quality of the anisotropically etched fluidic structures in silicon of the single channel approach.

By gravimetrical measurement of 1,000 shot salves of deionized water, an average dispensed droplet volume of V=10.0 pl was determined. Thereby the masses of the dispensed salves from one single chip deviate not exceeding a CV=24 % within a maximum range of $V_{drop,max}$–$V_{drop,min}$=7.5 pl.

Predominantly, the worse reproducibility is caused by irregularities in the fluidic structures in the TMMF layer.

It is obvious that the performance of the silicon based single channel approach is not reached by the polymer based setup. Nevertheless, the miniaturization potential of the polymer based fabrication cannot be dismissed. Utilizing more or less the same space, a setup that features up to four different channels can be realized by combining two double channel release cartridges face to face. It has to be mentioned that the presented application of the dry-film resist TMMF challenges the fabrication yield drastically. Whereas for the silicon based setup with anodic bonding rolled throughput fabrication yields (*RTY*) of *RTY*>70 % were achieved instantly, the utilization of polymer based fluidic structures reduced the fabrication yield to values below *RTY*=5 %. It should be mentioned that up to 232 chips are arranged on a 100 mm silicon wafer.

To summarize fabrication and the characteristics of the two different agent release cartridges, the main differences are depicted within Table 1 comparing the two approaches. Additional data concerning the characteristics are given in Online Resource 1.

3 Biological applications

Both approaches, the single and the double channel agent release cartridge feature the possibility of distinct and defined release of small amounts of highly effective agents. The agents can be directed to a well-defined position with a high spatial resolution (aiming accuracy radius Δr <50 μm for 700 μm distance). This is shown by the subsequent described experiments.

Table 1 Comparision table of single channel and double channel agent release cartridge

	Single channel agent release cartridge	Double channel agent release cartridge
Design / fabrication		
• Size	10×1.5×1 mm³	8×1.4×0.7 mm³
• Base-substrate	Pyrex glass	Silicon
• Fluidic structure material	Silicon (DRIE etched)	TMMF dry-film reisist
• Assembling technique	Anodic bonding	Lamination
• Reservoir volume	1×1 μl @ silicon top- substrate	2×1 μl @ silicon base- substrate
• Fabrication yield	*RTY* >70 %	*RTY*=5 %.
Dispensing characteristics		
• Actuation parameters	U_{act}=8.2 V, I_{act}=330 mA, t_{act}=2.5 μs, f=1000 Hz	U_{act}=9.0 V, I_{act}=330 mA, t_{act}=2.5 μs, f=1000 Hz
• Droplet volume	V_{drop}=15.1 pl	V_{drop}=10.0 pl
• Variation coefficient	CV=4.4 %	CV=24 %
• Spreading angle	β=3°	β=4°
• Chip-chip variation	CV=12 %	CV=26 %
• Chip-chip deflection from main shooting axis	α=5°	α=15°

3.1 Premature bud formation of Physcomitrella patens

Hormones play a major role in development and differentiation of *Physcomitrella patens* cells (moss) (Decker et al. 2006). The first days after germination of a spore, the protonema consists of chloronema cells. After approximately 6 days the hormone auxin (indole-3-acetic acid, IAA) causes differentiation into caulonema cells. Later on, the exposure to the hormone cytokinin (N6-isopentenyladenine) leads to bud-formation after an additional duration of 7 to 14 days (Reski 1998).

A single channel agent release cartridge with 10 μM cytokinin solution in Knop cell culture medium (water based saline nutrition solution) (Reski and Abel 1985) was positioned next to a selected target point of the protonema filament of *P. patens*, embedded in low-melting-point agarose gel. The covering Knop cell culture medium has been removed from the culture before application of ~6 nl cytokinin solution (2× 200 shots) at the target site and after 6 days, the filaments have been covered with Knop cell culture medium again to enable further development of the moss. So the cytokinin solution had the chance to incubate 6 days at the target site.

In several independent experiments, performed under same conditions, it had been shown that via the application of cytokinin premature bud formation was induced. As depicted in Fig. 4 and as proofed by negative controls the bud formation was only induced on the treated position and not elsewhere in the protonema.

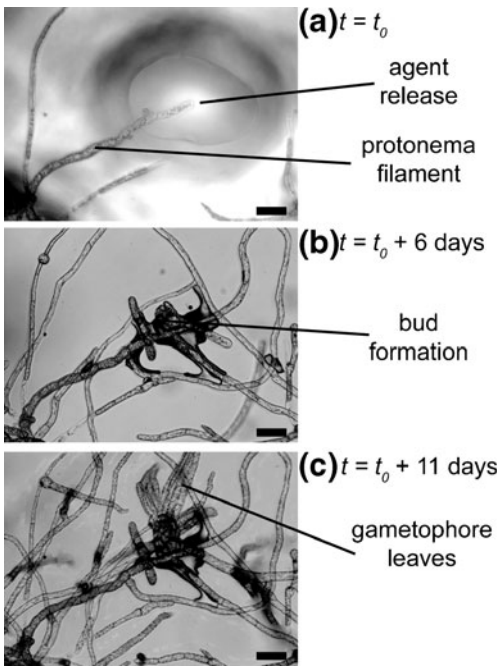

Fig. 4 Premature bud formation of *Physcomitrella patens* filaments. (**a**) At $t = t_0$ cytokinins are released to target site on the protonema filament. (**b** + **c**) After 6 days, a clear bud formation took place at the impingement site resulting in gametophore leave growing after 11 days. The scale bars represent a distance of 200 μm

3.2 Specific single cell staining

In a similar manner, single cells can be stained by using the agent release cartridge. To achieve a staining of the target cell within the cell culture, a steep concentration profile has to be generated by applying the agent as close as possible to the target cell.

Thereby, a distinct separation of the liquid cell culture medium that covers the cells for nutrition on the one side and the liquid agent within the dispenser nozzle on the other side is mandatory. Otherwise, diffusion would lead to an unpredictable agent leakage whenever the agent release cartridge comes in contact with the cell culture medium. In the manner of Steigert et al. a hydrophobic diffusion barrier has been realized by placing a disposable PDMS cap on top of the cartridge tip. Thereby, the cap generates a phase-gap between dispensing agent and target liquid when the dispenser is dipped into the latter (Steigert et al. 2009).

For the purpose presented here, a double channel release cartridge was filled with a fluorescent dye (lipopeptide coupled to Rhodamine from *EMC microcollections GmbH*, Tübingen, Germany (EMC microcollections 2011)) dissolved in Dulbecco's Modified Eagle Medium (DMEM). The agent release cartridge was positioned next to a selected L 929 cell (mouse fibroblast) (Drexler et al. 2001). A single shot of V=(10.0±2.6) pl was applied within the cell culture medium and the distribution of the fluorescent dye was monitored online by an inverted microscope (Fig. 5(a)) and the concentration profile was extracted (grey bar, Fig. 5(a)) as depicted in Fig. 5(b).

The distribution of the intensity profile can be approximated using Fick's 2nd law, solved with a Dirac's delta function at t=0 s (Eq. 1):

$$I(t,r) = I_{back} + \frac{I_0}{\sqrt{(4\pi \cdot D \cdot (t+t_0))^3}} e^{-\frac{r^2}{4 \cdot D \cdot (t+t_0)}}$$

where I_{back} defines the background fluorescence intensity, I_0 an initial fluorescence intensity within an infinite small volume. D describes the diffusion coefficient, r the radius from the impingement site, t the time of diffusion of the system and t_0 a temporal offset to mimic the initial droplet dimension.

The analytic model (Eq. 1) was fitted to the experimental data as shown in Fig. 5(b), using a non-linear least-squares approach (gnuplot). Here, the error of the experimental data was derived from background noise analysis. Best match was found for D=(71.1±0.5) μm^2/s and t_0=(0.45±0.02) s, resulting in χ^2=2.26.

However, it should be considered that a three-dimensional model is fitted to a two-dimensional projection of the fluorescent image in this case. A systematic error is thus inevitable here. Nevertheless, the experimentally derived diffusion coefficient of $D_{lipopeptide+Rhodamine}$=(71.1±0.5) μm^2/s is

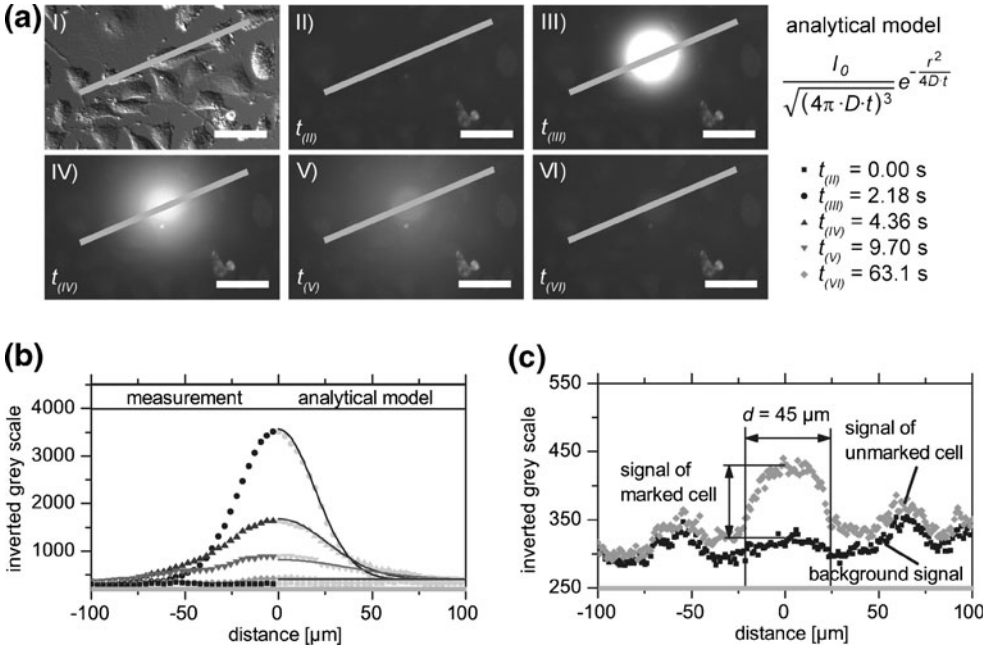

Fig. 5 Single cell staining within a confluent grown cell culture of L 929 cells. (**a**) Releasing one single agent droplet (V=10.0 pl±2.6 pl) (III) and investigation of the diffusion of the agent (III-VI). The agent acts on the target cell in a sharp concentration profile. The distribution follows an analytic model based on Fick's diffusion (**b**). After reaction of the fluorescent dye with the target cell, the cell is stained significantly whereas neighbor cells are negligibly influenced by the dye application (**c**). The scale bars represent a distance of 50 µm

in the right order of magnitude and shows a realistic value, comparing the well-known diffusion coefficient of Rhodamine ($D_{Rhodamine\ B}$=360 µm^2/s (Rani et al. 2005)) and the sizes of the used molecules to the estimated results ($Ø_{lipopeptide+Rhodamine} >> Ø_{RhodamineB}$) (Wangler et al. 2009).

With the achieved concentration profile, the concentration at the release site decreases drastically within 8 s (c <1/5 c_{max}). Furthermore, the concentration profile never exceeds 1/5 c_{max} outside a radius r=50 µm and due to its chemical similarity to natural cell membrane lipopeptide as described by Brown (Braun and Rehn 1969), the Rhodamine lipopeptide integrates into the L 929 cell membranes instantaneously. After 1 min, the target cell emits a fluorescent signal as depicted in Fig. 5(c) and a distinction between the labeled cell and its neighbors is possible. An increase in the fluorescence signal of the stained cell of more than 100 grey scale values can be recognized within the presented experiment. Regarding the difference in the fluorescence signal before and after staining, a difference threshold value of 100 grey scale values can be used for an automated detection of stained cells for example. Since the fluorescence signal depends of the imaging procedure (e.g. exposure time, binning mode), such a threshold value has to be defined for each experiment anew.

4 Conclusions

The Bubble-Jet dispensing technology enables drop-on-demand agent release of small picolitre volumes with a small and easy to handle device. Therefore, this technology is predestined for the application in chemical single cell stimulation. Droplets in the size of the cell diameter can be applied on specified target sites to stimulate or manipulate single cells or small cell clusters.

We presented two fabrication routes for the realization of an agent release cartridge that features the actuation unit, fluidic channels, and integrated reservoirs. In a first approach the fluidic channels and nozzle structures were etched into silicon by deep reactive ion etching. The silicon wafer is bonded to a Pyrex substrate, featuring the Bubble-Jet actuation unit. The approach led to high fabrication yield, but due to limitations in anodic bonding the pitch between two separated channels is limited to about 300 µm.

In a second approach a double channel agent release cartridge was fabricated with fluidic channels and nozzle structures made of the epoxy-based dry film photoresist TMMF. While with the silicon/Pyrex based approach a fabrication yield of RTY >70 % and intra-chip volume accuracies of CV <5 % were realized, for the TMMF based approach the fabrication yield dropped down to 5 % and for the properly operating dispensers the intra-chip volume variations may exceed CV=20 %. Consequently, for an efficient use, the TMMF based approach requires further optimization of fabrication process.

Nevertheless, both setups are feasible for the specific chemical stimulation of small cell clusters or single cells. This is shown by the premature cell differentiation of *Physcomitrella patens* cells by the aimed application of phytohormones and the specific staining of one single L 929 cell in a confluent grown cell culture.

For the application of the agent release cartridge within a liquid cell culture medium, a distinct separation of liquid culture medium and agent within the nozzle is necessary. This can be realized by attaching a hydrophobic cap onto the dispensers tip. Agent release is thus

performed by shooting the agent droplets through a captured air bubble onto the target site.

With this work, a new tool for specific chemical stimulation of individual single cells is presented. Utilizing the new agent release cartridge, single cells or small cell clusters can be stimulated or manipulated in their natural growing environment. There is no need of growing the cells on sophisticated setups that might influence the behavior of the cells. As demonstrated here, even the precise application on cells in real natural environment like in the moss filament (protonema) is possible, thus facilitating the targeted perturbation of internal hormonal gradients.

Acknowledgments We gratefully thank the German Research Foundation (DFG, ZE 527/4 and EXC 294) for financial support of this project. We also appreciate the good cooperation with the Cleanroom Service Center at IMTEK.

References

H. Andersson, A. van den Berg, Lab. Chip **4**(2), 98–103 (2004)
H. Andersson, A. van den Berg, Lab. Chip **7**, 544–546 (2007)
T. Boland, T. Xu, B. Damon, X. Cui, Biotechnol. J. **1**, 910–917 (2006)
S. Boyden, J. Exp. Med. **115**(3), 453–466 (1962)
V. Braun, K. Rehn, Eur. J. Biochem. **10**, 426–438 (1969)
Cellectricon, Dynaflow®Pro II System – High Quality Automated Patch Clamping (Cellectricon AB, Mölndal, Sweden). http://www.cellectricon.se. Accessed Feb. 2011
B. Dadacz-Narloch et al., Plant Cell **23**, 2696–2707 (2011)
E.L. Decker, W. Frank, E. Sarnighausen, R. Reski, Plant Biol. **8**, 397–405 (2006)
H.G. Drexler, et al. *DSMZ Catalogue of Human and Animal Cell Lines*, Eighth Edition. (2001)
U. Egert et al., Brain Res. Protocol. **2**, 229–242 (1998)
J. El-Ali et al., Anal. Chem. **77**, 3629–3636 (2005)
R. Elmqvist, Measuring instrument of the recording type, US Patent 2566443, 1951
Eppendorf, Microinjectors FemtoJet and FemtoJet express Product Sheet (Eppendorf AG Hamburg, Germany). http://www.eppendorf.de. Accessed Feb. 2011
P. Jonas, Fast application of agonists to isolated membrane patches. In *Single-Channel Recording*, eds. B. Sakmann & E. Neher (Plenum press, 1995), pp. 231–243
T.M. Keenan, A. Folch, Lab. Chip **8**, 34–57 (2008)
T. Kraus et al., Lab. Chip **6**, 218–229 (2006)
H.P. Le, J. Imag. Sci. Tech. **42**, 49–62 (1998)
L. Leoni, D. Attiah, T.A. Desai, Sensors **2**, 111–120 (2002)
X. Liu et al., (IEEE Trans. Rehabil. Eng. **7**(3), 315–326 (1999)
J. Noolandi et al., Biomed. Microdev. **5**(3), 195–199 (2003)
Pam3Cys-SKKKK(Rhodamin), (EMC microcollections GmbH, Tübingen, Germany). http://www.microcollections.de. Accessed Feb. 2011
M.C. Peterman, J. Noolandi, M.S. Blumenkranz, H.A. Fishman, PNAS **101**(27), 9951–9954 (2004)
S.A. Rani et al., Antimicrob. Agents Chemother. **49**(2), 728–732 (2005)
R. Reski, Botanica Acta **111**, 1–15 (1998)
R. Reski, W.O. Abel, Planta **165**, 354–358 (1985)
E.A. Roth, T. Xu, M. Das, C. Gregory, J.J. Hickman, T. Boland, Biomaterials **25**, 3707–3715 (2004)
J. Steigert et al., Lab. Chip **9**(12), 1801–1805 (2009)
U. Stöhr, P. Vulto, P. Hoppe, G. Urban, H. Reinecke, Journal of Micro/Nanolithography, MEMS, and MOEMS. **7**, 033009 (2008)
S. Takayama, E. Ostuni, P. Leduc, K. Naruse, D.E. Ingber, G.M. Whitesides, Nature **411**(6841), 1016 (2001)
D.A. Wagenaar, J. Pine, S.M. Potter, J. Neurosci. Met. **138**, 27–37 (2004)
N. Wangler et al., *Proceedings of Thirteenth International Conference on Miniaturized Systems for Chemistry and Life Sciences November 1–5.* (2009), 679–81
N. Wangler et al., J. Micromech. Microeng. **21**(095009), 9 (2011)
S. Zibek et al., Biophys. J. **92**(1), L04–L06 (2006)